

## Misfire Detection in a Dynamic Skip Fire Engine

S Kevin Chen, Li-Chun Chien, Masaki Nagashima, Joel Van Ess, and Sam Hashemi  
Tula Technology Inc.

### ABSTRACT

Misfire detection and monitoring on US passenger vehicles are required to comply with detailed and specific requirements contained in the OBD-II regulations. Numerous technical papers and patents discuss various methods and metrics for detecting misfire in conventional all-cylinder firing engines. However, the current methods are generally not suitable for detecting misfires in a dynamic skip fire engine. For example, a detection approach based on peak crankshaft angular acceleration may work well in conventional, all-cylinder firing engine operation, since it is expected that crankshaft acceleration will remain generally consistent for a given operating condition. In a skip fire engine, any cylinder or cycle may be skipped. As a result, the crankshaft acceleration peaks and profiles may change abruptly as the firing sequence changes. This paper presents two approaches for detecting misfires in a dynamic skip fire engine.

The first method utilizes crankshaft angular acceleration with the addition of cylinder skip or fire status, which is used to recognize a firing sequence in order to ignore skips and apply a separate threshold to various sequences. For the second approach, a torque model based on multi-cylinder pressure modeling is employed. The paper describes the details in modeling cylinder pressure, indicated torque and crankshaft angular acceleration, and proposes a new metric for misfire detection. Validation tests are carried out both on an engine dynamometer and a vehicle under steady state and transient conditions. The results indicate a very promising approach for detecting misfires in a dynamic skip fire engine.

**CITATION:** Chen, S., Chien, L., Nagashima, M., Van Ess, J. et al., "Misfire Detection in a Dynamic Skip Fire Engine," *SAE Int. J. Engines* 8(2):2015, doi:10.4271/2015-01-0210.

### INTRODUCTION

A dynamic skip fire engine has the ability to selectively deactivate cylinders, in which any cylinder or cycle may be skipped to match the torque demand. This strategy improves fuel economy significantly by minimizing pumping losses while only a few cylinders operate at their peak efficiency to deliver torque. To illustrate this concept, [Figure 1](#) shows firing density versus torque demand. As the torque demand increases, the density of firing cylinders also increases. Design considerations and benefits of dynamic skip fire engines are presented in SAE papers [1] and [2].

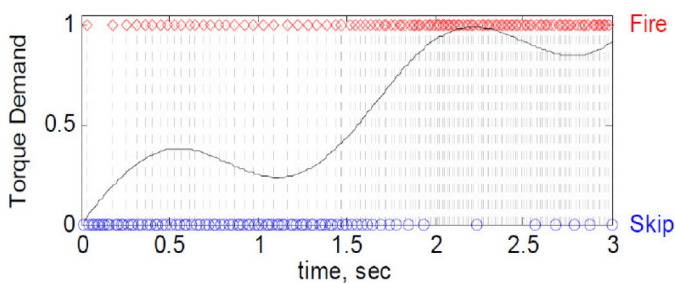


Figure 1. Dynamic skip fire concept

Integrating dynamic skip fire into an engine control strategy greatly impacts on-board diagnostic systems, particularly on misfire detection. There have been a number of methods available to detect misfires on conventional all-cylinder firing spark-ignition engines [3]. A recent SAE paper compares various misfire detection technologies for such engines [4]. Crankshaft angular acceleration has long been used for misfire detection for internal combustion engines [5]. Other methods using the signal of a knock sensor [6] or a torque model [7, 8], have also been proposed. For conventional all-cylinder firing engines, these approaches provide a reasonably accurate means for misfire detection. The methods rely on the fact that angular acceleration is proportional to torque and that neighboring cylinders produce similar torque for a given engine operating condition. Misfire of a particular cylinder results in reduced torque for that cylinder. In a conventional engine, this reduced torque and corresponding reduced angular acceleration can be used to determine a misfire.

In a skip fire engine, a particular cylinder may be skipped instead of fired, which results in a missing torque pulse or low angular acceleration. Since the lack of torque production is equivalent to a misfire, this makes it difficult to discern a misfire from a skip when looking only at angular acceleration. Thus information on whether a cylinder is fired or skipped needs to be explicitly considered. When a cylinder is skipped, no effort is made to detect a misfire event with respect to that specific cylinder. In this way, the lack of acceleration

peaks during the time period or crank angle window associated with the skipped firing opportunities will not be interpreted as misfires of the associated cylinders.

Additionally, the firing sequence needs to be identified in order to apply a different threshold to different firing sequences due to the effects of fire/skip operation of neighboring cylinders. In a more sophisticated implementation the acceleration threshold is determined dynamically by the output of a torque model based on the known sequence of fires and skips, and cylinder loading, via their resulting modeled torque waveform.

## EXPERIMENTAL SETUP

The development of misfire detection on a skip fire engine was carried out on two GMC Yukon Denali full-size sport utility vehicles, each equipped with a 6.2L port fuel injected V8 engine, and with an engine on an eddy-current dynamometer. The Dynamic Skip Fire (DSF) engine was based on a production engine with GM's Active Fuel Management (AFM) system, which deactivates four out of the eight cylinders. The valvetrain of the engine and the engine controller were modified so that the test engine is capable of deactivating all eight cylinders. The specifics of this engine are listed in Table 1. Additional information on engine modifications performed can be found in [1].

Table 1. Engine and transmission specifications

Engine Designation	GM L94
Displacement	6.2 Liters
Engine Configuration	V8
Power	406 hp
Transmission	6 Speed Automatic
Valvetrain	2 Valve per cylinder, Single Cam
Cylinder Deactivation	8 cylinders, individually controlled

The engine is controlled by a dSPACE engine control unit comprised of a RapidPro and MicroAutobox. This controller allows the engine to be operated in a normal mode of pedal torque request to produce vehicle acceleration or cruise accordingly. The engine controller also has the ability to specify any firing density or firing sequence under steady state or transient conditions. This allows test data to be collected at all engine operating conditions for model development and validation.

Misfire generation code was developed for the controller to allow simulated misfires to be induced at any specified frequency at any given cylinder, two sequential cylinders, or two opposing cylinders. Misfires are simulated by not injecting fuel for a cylinder that is otherwise scheduled to fire. This approximates misfire from a torque and valve state standpoint. By programming misfires this way, the catalyst is protected from potential damage by avoiding large amounts of unburnt hydrocarbons flowing into the converter.

In initial experiments the engine is operated on an eddy current dynamometer test cell which has extensive instrumentation including piezoelectric in-cylinder pressure transducers, intake runner pressure

transducers, and a high resolution crankshaft encoder used by a combustion analysis system to analyze peak cylinder pressures and indicated mean effective pressure (IMEP). The transducers and piezo amplifiers are made by AVL, Kistler and Kulite, and the data acquisition system is from A&D. The data collected on the dynamometer can be correlated with results from the cylinder pressure model and torque model for validation.

Due to the possibility of programmed misfires producing resonance on the engine dyno driveshaft not indicative of those on the vehicle, as well as the lack of a slipping torque converter and torque converter clutch, further development and validation of misfire detection is carried out using test vehicles on the road. These are production vehicles with only engine and the engine controller modifications to be able to deactivate all eight cylinders, as described earlier. Spark plug pressure transducers and combustion analysis system were fitted in the vehicle to validate the cylinder pressure model when needed. The engine speed signals, based on which the crankshaft angular acceleration is calculated, are generated from the production 60-2 tooth crank trigger wheel. The vehicles were driven at steady state or on transient cycles for functionality validation. The data is saved as Matlab files and processed using in-house developed scripts.

## RESULTS AND DISCUSSION

A number of misfire detection techniques were explored during development. This paper describes the two most promising methods. Both methods use the production vehicle sensor set and thus do not add cost.

### A. Angular Acceleration with 3-Cylinder Firing/Skip Status

In general, engines having multiple cylinders are designed with their cylinders working out of phase with one another at consistent intervals, such that the power stroke of one cylinder occurs during the compression stroke of the next cylinder. Figure 2 illustrates torque signatures for three sequential cylinders with relative phasing corresponding to an 8-cylinder engine. Fired, skipped, and misfire torque signatures are depicted, with the skipped cylinder operating as with low-pressure exhaust trapping strategy.

The shaded area between 270 and 360 crank angle degrees indicates that Cylinder N is in the first half of power stroke, the previous cylinder (Cyl N-1) is in the second half of power stroke while the next cylinder (Cyl N+1) is in the second half of compression stroke. This illustrates that crank acceleration or torque in the shaded window where misfire detection occurs for the cylinder of interest (Cyl N), can be significantly affected by the events occurring in the adjacent cylinders. Although the other cylinders have a small torque effect executing their intake or exhaust processes, the influences from the immediately adjacent cylinders in the firing order are most significant and account for majority of the torque effects.

Figure 2 also shows that the commanded firing status (fire or skip) in the cylinder before (Cyl N-1) and the cylinder after (Cyl N+1) the cylinder of interest has a different effect on the crank acceleration or torque during the detection window. In a conventional, all-cylinder

firing engine, the cylinders N-1 and N+1 are always firing, therefore the effect on torque is consistent. In a fixed pattern cylinder deactivation engine, such as four out of eight cylinders deactivated, Cylinders N-1 and N+1 are both normally skips. Therefore, the effect on torque signature from Cylinders N-1 and N+1 is also consistent from cycle to cycle under quasi-steady state conditions. However, in a dynamic skip fire engine, the fire/skip status of the cylinders N-1 and N+1 are changing dynamically. Therefore, it is important that the fire/skip status of both Cylinders N-1 and N+1 are taken into consideration in the misfire detection algorithm design. This is why a 3-cylinder pattern was chosen for this method.

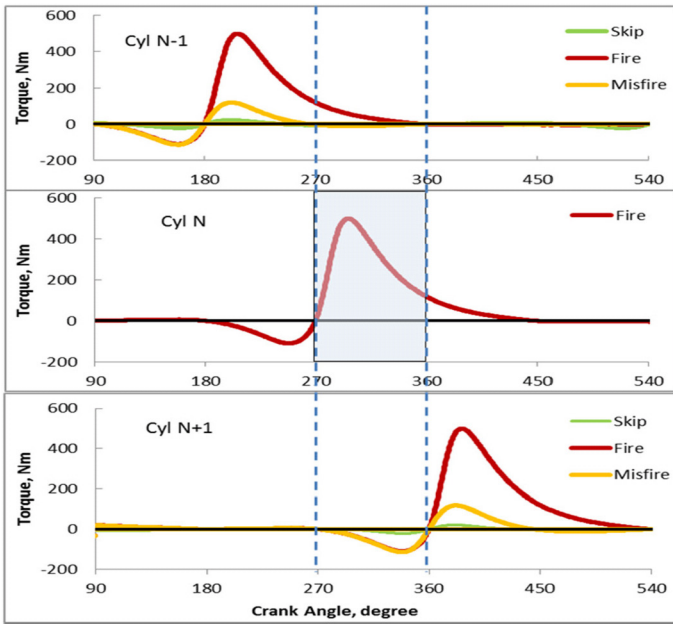


Figure 2. Effect of adjacent cylinders on crankshaft torque

Figure 3 below depicts a flow diagram of the 3-cylinder status based misfire detection algorithm in a DSF engine. It should be noted that if the previous cylinder was commanded to fire, but a misfire has been detected in that cylinder, then both misfire flag and the fire status should be taken into account since the torque contribution from that cylinder during the detection window is greatly reduced, as illustrated in Figure 2 above. It should also be pointed out that the algorithm performs rationality checks on input signals to ensure robustness of the strategy.

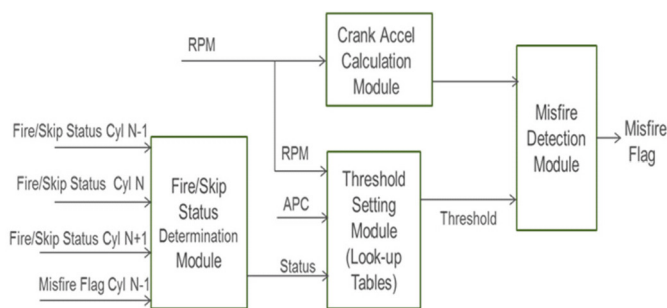


Figure 3. A flow diagram illustrating misfire detection algorithm based on 3-cylinder fire/skip status

### Crank Acceleration Calculation Module

The angular crank acceleration is calculated in the Crank Accel Calculation module. The calculation is performed over a 90-degree moving window and is updated every 6 degrees (every crank tooth), as depicted in Figure 4A. The 90-degree window is further divided into two segments, each of 42 degrees and separated by a 6-degree gap. The purpose in doing so is to frequency band-limit the detection area to exclude noise sources outside of the frequency of where the bulk of the combustion event is located. This is important since angular acceleration is the derivative of the angular velocity and a derivative function is essentially a high pass filter that would otherwise pass high frequency noise that might confound the detection of misfire. The calculated angular acceleration is then latched for each cylinder in a 90-degree interval for an 8-cylinder engine, as illustrated in Figures 4B and 4C. It should be pointed out that this 90-degree latching interval derives from the 720 crank angle degrees per cycle divided by the number of cylinders of the engine and does not necessarily have to be the same as 90-degree filtering window.

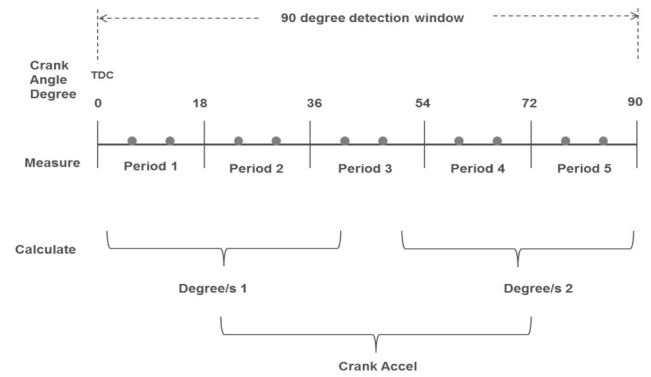


Figure 4A. Method of calculating crankshaft angular acceleration

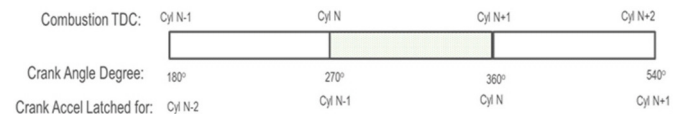


Figure 4B. A diagram illustrating location for latching crankshaft angular acceleration

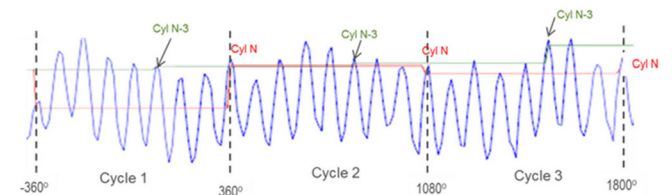


Figure 4C. Example of results of calculated crankshaft angular acceleration

### Fire/Skip Status Determination Module

As discussed earlier, the fire/skip status of the two cylinders immediately adjacent to the cylinder of interest (Cyl N) has significant impact on crank acceleration in the detection window. To categorize the eight different possible combinations of fire/skip statuses of Cylinders N-1, N and N+1, the following definition is employed and the results are summarized in Table 2:

$$3\text{-Cylinder Status} = S_{N-1} * 2^2 + S_N * 2^1 + S_{N+1} * 2^0 \quad (1)$$

However, it is recognized that if the cylinder of interest is a skip, as in subgroups with the 3-cylinder status of 5, 4, 1, and 0, misfire detection is not required. As a result, Table 2 shows there are only six possible scenarios, labeled as Groups 1, 1A, 2, 2A, 3, and 4, respectively, where the cylinder of interest is commanded to fire and will be monitored for potential misfire.

Table 2. Possible combinations of fire/skip statuses of 3 cylinders

Misfire Group #	Status @ Cyl N-1	Status @ Cyl N	Status @ Cyl N+1	3-Cylinder Status
Group 1 Group 1A	Fire (S=1) Misfire (S=1)	Fire (S=1)	Fire (S=1)	7
Group 2 Group 2A	Fire (S=1) Misfire (S=1)	Fire (S=1)	Skip (S=0)	6
N/A	Fire (S=1)	Skip (S=0)	Fire (S=1)	5
N/A	Fire (S=1)	Skip (S=0)	Skip (S=0)	4
Group 3	Skip (S=0)	Fire (S=1)	Fire (S=1)	3
Group 4	Skip (S=0)	Fire (S=1)	Skip (S=0)	2
N/A	Skip (S=0)	Skip (S=0)	Fire (S=1)	1
N/A	Skip (S=0)	Skip (S=0)	Skip (S=0)	0

### Threshold Setting Module

The Threshold-Setting module determines crank acceleration threshold based on engine speed (RPM) and air charge per cylinder (APC). It is noted that intake manifold pressure (MAP) has typically been used to determine misfire detection threshold for conventional all-cylinder firing engines, since MAP is generally proportional to torque generated by the engine. However, for a dynamic skip fire engine, it is recommended to use air charge per cylinder (APC) for index of the threshold look-up tables since APC is a better indicator of amount of torque produced per cylinder. To calibrate the look-up tables, crank acceleration data is acquired on the test vehicles under different firing densities with and without induced misfire. The data is then sorted into six different groups based on the 3-cylinder status value discussed above. Therefore, six different RPM & APC based look-up tables can be constructed to provide threshold values to determine misfire. It is possible that an adaptive algorithm can be incorporated to update the calibration values on the table based on real-time calculation of crank acceleration under the real-world driving conditions.

### Misfire Detection Module

The Misfire Detection module compares calculated crank acceleration to an appropriate threshold value from one of the lookup tables and generates a misfire flag when the threshold is exceeded. The comparison is performed only for a cylinder that is scheduled to fire, since a deactivated cylinder obviously has no misfire to detect. The misfire flag generated by this module can also be used to initiate any remedial action if the frequency of misfire exceeds a certain threshold. For a dynamic skip fire engine,

additional options for remedial actions are available, such as deactivation of the cylinder in addition to fuel cut-off to avoid pumping un-combusted air into the exhaust.

The probability of detection is defined as percentage of misfire detected for a given number of induced misfires. The algorithm has been developed on the two test vehicles, either on a chassis dynamometer or on the road. Data at various speed and load conditions was collected to develop thresholds for the look-up tables. Figure 5 shows an example of the data obtained while driving on the road at approximately 45 mph at 1500 rpm. As illustrated on the graph, there is comfortable separation between crank acceleration with and without misfires for four groups. Under most speed load points, the algorithm has been demonstrated to achieve over 95% probability of detection.

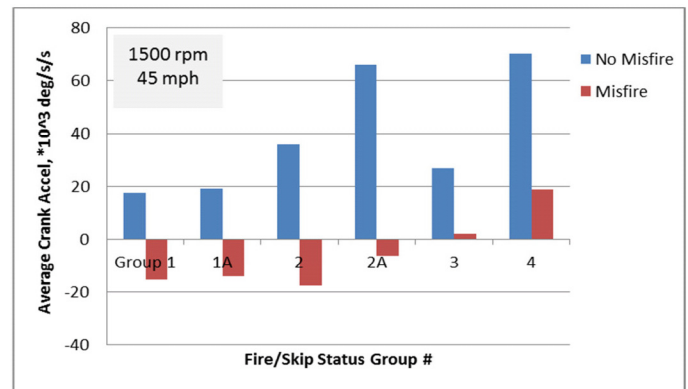


Figure 5. Example of crank angular acceleration of 4 different groups with and without induced misfires

### B. Cylinder Torque Model Based

Although the angular acceleration with 3-Cylinder Status based method has been demonstrated to be effective in detecting misfire in most speed and load regions, significant calibration effort is needed to create thresholds for all possible engine operating conditions and firing patterns of a dynamic skip fire engine. To minimize the calibration burden, an alternative approach has been explored. The second method described in this paper uses a cylinder pressure model to calculate a nominal crankshaft angular acceleration. This detection method relies on the comparison of expected angular acceleration calculated from cylinder pressure to measured angular acceleration from the crankshaft position sensor. Figure 6 is a flow diagram illustrating the steps involved in this methodology. It should also be noted that input signal rationality checks are performed in each module, in order to determine integrity of input signals to ensure robustness of the strategy.

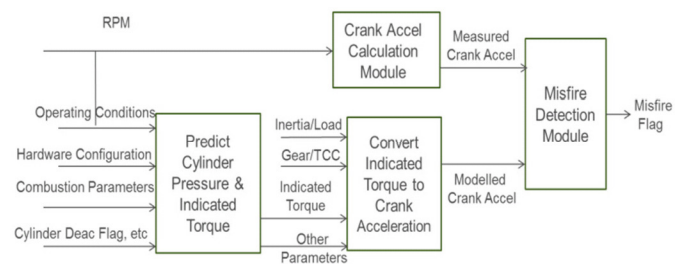


Figure 6. A flow diagram illustrating cylinder torque based misfire detection algorithm

### Crank Acceleration Calculation Module

The crankshaft angular acceleration is calculated in the same way as described previously under 3-Cylinder Status based method.

### Predicting Cylinder Pressure and Torque

An analytical cylinder pressure model based on an ideal Otto cycle was developed following the approach of [9]. The model predicts pressure in each cylinder not only during the combustion phase but also during skipped cycles. The modelled cylinder pressure is then used to calculate the indicated torque based on a simple crank-slider mechanism [10].

#### Pressure Model Description

A main concept of the analytical pressure model in [9] assumes that the cylinder pressure  $p(\theta)$  modeled as the interpolation between two asymptotic pressure traces as illustrated in Figure 7 below.

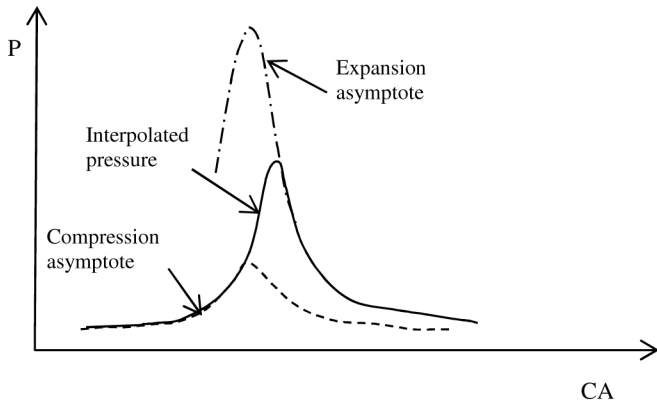


Figure 7. Interpolation method of cylinder pressure between two asymptotes [9]

The compression stroke is modelled by a polytropic process characterized by a polytropic exponent  $k_c$  and the thermodynamic state at intake valve closing (IVC). The reference states at IVC are determined from experimental data. These traces determine the compression asymptote up until ignition. The expressions for pressure and temperature for this process are

$$p_c(\theta) = p_{IVC} \left( \frac{V_{IVC}}{V(\theta)} \right)^{k_c} \quad (2)$$

$$T_c(\theta) = T_{IVC} \left( \frac{V_{IVC}}{V(\theta)} \right)^{k_c-1} \quad (3)$$

The expansion asymptote is also described by a polytropic process with polytropic exponent  $k_e$ . The quantities  $p_3$ ,  $T_3$  and  $V_3$  correspond to point 3 in the ideal Otto cycle depicted in the P-V diagram shown in Figure 8.

$$p_e(\theta) = p_3 \left( \frac{V_3}{V(\theta)} \right)^{k_e} \quad (4)$$

$$T_e(\theta) = T_3 \left( \frac{V_3}{V(\theta)} \right)^{k_e-1} \quad (5)$$

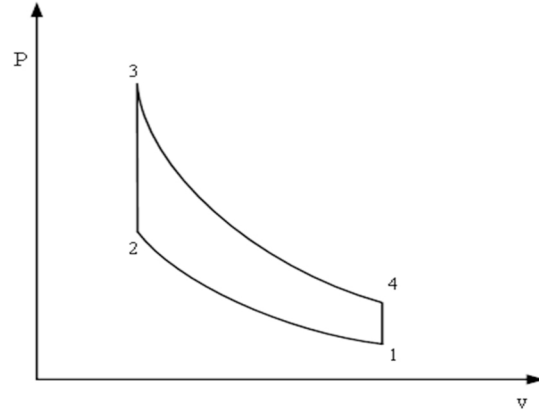


Figure 8. P-V diagram of an ideal Otto cycle

The temperature rise  $\Delta T_{comb}$  due to combustion is added to  $T_2$  and state of  $(P_2, T_2)$  can be obtained from equation (2) and (3).

$$T_3 = T_2 + \Delta T_{comb} \quad (6)$$

$$p_3 = p_2 \frac{T_3}{T_2} \quad (7)$$

$$\Delta T_{comb} = \frac{m_f q_{HV} \epsilon}{c_v m_{tot}} \quad (8)$$

Where fuel mass  $m_f$ , heating value  $q_{HV}$ , conversion efficiency  $\epsilon$ , specific heat  $c_v$ , and total mass  $m_{tot}$  are used.

The interpolation between two asymptotes is based on the pressure ratio approach described in [11] which is based on fitting heat release with the well-known Wiebe function described by parameters  $a$ , start of combustion angle  $\theta_{SOC}$ , combustion duration  $\Delta\theta$ , and exponent  $m$ , which are derived from experimental data. The pressure ratio is modelled by

$$PR(\theta) = 1 - e^{-a \left( \frac{\theta - \theta_{SOC}}{\Delta\theta} \right)^{m+1}} \quad (9)$$

This can then be used for the interpolation

$$p(\theta) = (1 - PR(\theta)) \cdot p_c(\theta) + PR(\theta) \cdot p_e(\theta) \quad (10)$$

The procedure above provides a simple and complete model for pressure between IVC and EVO. The pressure during gas exchange is set to the intake manifold pressure in [11]. However, for skipped cycles, the pressure will drop below intake manifold pressure. To properly model the pressure evolution during a skipped cycle, a

polytropic process referenced to the exhaust valve closing (EVC) was used. The pressure at EVC for firing cycles is derived from experimental data.

$$p(\theta) = p_{EVC} \left( \frac{V_{EVC}}{V(\theta)} \right)^{k_c} \quad (11)$$

A snapshot of the modelled pressure is shown below in Figure 9. The pressures during skipped cycles as well as the firing cycles are captured well enough for accurate torque prediction as described next.

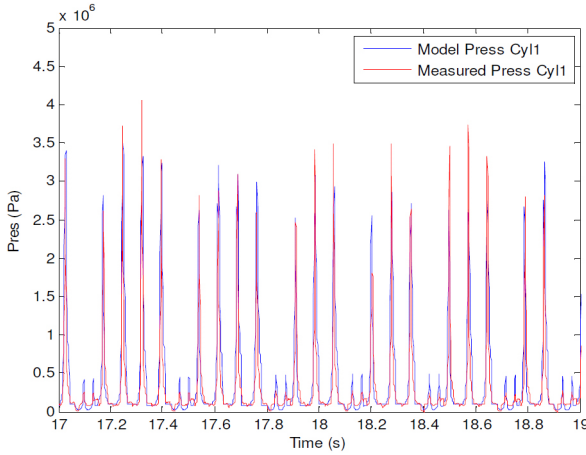


Figure 9. Comparison of measured and modelled cylinder pressure

### Indicated Torque

The gas force acting on a piston connected to the crank shaft by a rod with a crank slider mechanism produces at each instant an “indicated torque”

$$T_{cyl,i}(\theta) = (P_{cyl,i}(\theta) - P_{crank})Ar \frac{\sin(\theta+\beta)}{\cos\beta} \quad (12)$$

$$\beta = \sin^{-1} \frac{\delta+r \sin(\theta-\varphi)}{l} \quad (13)$$

$$\varphi = \sin^{-1} \frac{\delta}{(r+l)} \quad (14)$$

where  $P_{crank}$ ,  $r$ ,  $\delta$ ,  $l$  and  $A$  are crankcase pressure, crank radius, pin offset, connecting rod length and piston face cross-section area, respectively. The resultant engine indicated torque is just sum of the contributions from each cylinder.

$$T_i(\theta) = \sum_{Numcyl} T_{cyl,i}(\theta) \quad (15)$$

### Converting Torque to Crank Acceleration

The indicated engine torque obtained from the cylinder pressure model is used to determine crank angular acceleration. The engine dynamic model used for this derivation is

$$J_{eq} \ddot{\theta} + M_{eq} r^2 [f_1(\theta)\ddot{\theta} + f_2(\theta)\dot{\theta}^2] f_3(\theta) = T_i(\theta) - T_{fp}(\theta) - T_L(\theta) \quad (16)$$

where

$$f_1(\theta) = f_3(\theta) = \sin\theta + \frac{r}{2l} \sin 2\theta \quad (17)$$

$$f_2(\theta) = \cos\theta + \frac{r}{l} \cos 2\theta \quad (18)$$

$\theta$  is the crank angle,  $\dot{\theta}$  and  $\ddot{\theta}$  are the angular velocity and the angular acceleration of the crankshaft, respectively.  $l$  is the connecting rod length, and  $r$  is the crank radius.  $J_{eq}$  is the moment of inertia of the crankshaft, flywheel, gear and rotating part of connecting rod, and  $M_{eq}$  is the mass of the piston, rings, pin and linear motion part of the connecting rod.  $T_i(\theta)$ ,  $T_{fp}(\theta)$ , and  $T_L(\theta)$  are the indicated engine torque, friction torque, and load torque, respectively. The derivation of this equation can be found in the literature, for example [12].

The crank angle  $\theta$ , crank angular velocity  $\dot{\theta}$ , and equivalent mass  $M_{eq}$  are measured, and the indicated engine torque  $T_i(\theta)$  is given by the model described in the previous section. The friction torque  $T_{fp}(\theta)$  is determined by a lookup table obtained from experiments which relates the crank RPM to friction torque. The combined moment of inertia of crankshaft, flywheel, gear, and rotating part of connecting rod,  $J_{eq}$ , is also determined experimentally for each gear.

The load torque  $T_L(\theta)$  is estimated from the difference between the engine speed and turbine shaft speed through equation (19) for the torque converter and torque converter clutch [13].  $T_p$  is the torque converter torque and  $T_{tcc}$  is the torque converter clutch torque.  $K_i$  is calculated by a lookup table obtained from experiments and torque converter clutch gain  $K_{tcc}$  and a constant  $\alpha$  are also determined experimentally.

$$\begin{aligned} T_L &= T_p + T_{tcc} \\ T_p &= \frac{\omega_e - \omega_t}{|\omega_e - \omega_t|} \frac{\omega_e^2}{K_i^2} \\ T_{tcc} &= K_{tcc} \tanh\left(\frac{\omega_e - \omega_t}{\alpha}\right) \end{aligned} \quad (19)$$

$\omega_e$  and  $\omega_t$  are the angular speed of crankshaft and turbine shaft, respectively. In application, discrete-time low-pass filters are applied to  $T_p$  and  $T_{tcc}$  to remove high frequency components. The low-pass filter is given by the following transfer function

$$F(z) = \frac{b}{z-a} \quad (20)$$

where  $a$  and  $b$  are filter constants.

Equation (16) is solved for  $\ddot{\theta}$  using the measured crank angular velocity  $\dot{\theta}$  via

$$\ddot{\theta} = \frac{1}{J_{eq} + M_{eq} r^2 f_1 f_3} [-M_{eq} r^2 f_2 f_3 \dot{\theta}^2 + T_i(\theta) - T_{fp}(\theta) - T_L(\theta)] \quad (21)$$

When misfire occurs, the measured  $\dot{\theta}$  contains the effect of misfire and strictly speaking, measured  $\dot{\theta}$  should not be used to obtain  $\ddot{\theta}$  from the model. But the effect is considered to be negligible for the purpose of misfire detection.

### Filtering of Crank Acceleration

The crank acceleration obtained from the model needs to be compared with the measured crank angular acceleration. Measured crank acceleration is computed from the measured crank angular speed in the 6-degree angle domain, where the crank angular speed is sampled at every 6 crank angle degrees, by the following formulae to reduce the effect of measurement noise.

$$A_{time}(n) = \frac{\sum_{k=1}^7 T_d(n-k) - \sum_{k=9}^{15} T_d(n-k)}{\sum_{k=4}^{10} T_d(n-k)} \quad (22)$$

$$T_d(n) = \frac{6}{360 \cdot \frac{r(n)}{6}} = \frac{1}{10} \frac{1}{r(n)} \quad (23)$$

$r(n)$  is the crank angular speed at time step  $n$  in 6 degree angle domain. The acceleration formulae (22) can also be approximated as the double average of acceleration shown below.

$$A_{rpm}(n) = \frac{\frac{1}{7} \sum_{k=1}^7 r(n-k) - \frac{1}{7} \sum_{k=9}^{15} r(n-k)}{\sum_{k=4}^7 T_d(n-k)} = \frac{1}{7} \sum_{k=1}^7 \frac{1}{7} \sum_{m=0}^6 a(n-k-m) \quad (24)$$

Here the term  $T_d(n)$  is treated as a constant during the time steps considered and Euler's rule is used to derive the relationship between  $r(n)$  and the acceleration  $a(n)$ . Figure 10 shows comparison of the two averaging methods (22) and (24) applied to the same angular speed signal generated for validation purposes. It can be verified the difference between the two methods is negligible. This comparison demonstrates that the acceleration obtained from the engine dynamics model can be filtered in 6-degree domain and can be compared with the measured acceleration obtained from (22).

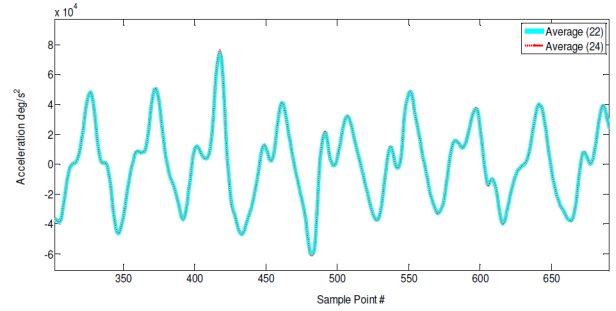


Figure 10. Comparison of crank acceleration averaging methods

A high-pass filter is then applied to both double-average filtered measured and modelled accelerations. The high-pass filter removes the mean value offset errors in the torque estimate, making it easier to compare the characteristics of the measured and simulated accelerations relevant for misfire detection. The high-pass filter is given by

$$y(z) = -a_1 y(n-1) - a_0 y(n-2) + b_2 x(n) + b_1 x(n-1) + b_0 x(n-2). \quad (25)$$

Where,  $a_0, a_1, b_0, b_1$  and  $b_2$  are the appropriate filter coefficients determined by experimental data.

### Misfire Detection Module

The Misfire Detection module compares the crank acceleration obtained from measured angular velocity (based on periods between two teeth on the crank wheel) to the crank acceleration obtained from the model described above to determine whether a misfire has occurred. To achieve that, a new parameter, called Misfire Detection Metric (MDM), is introduced and is defined as:

$$MDM = \left( \frac{CrankAccel_{modelled} - CrankAccel_{measured}}{APC} * C - A \right)^3 \quad (26)$$

Where APC is mass of air charge per cylinder in mg/stroke, C is a normalizing factor to make MDM dimensionless and A is a constant to bias the signal. The result is then raised to the power of 3 to amplify the signal to noise ratio.

By using this normalized metric, the threshold no longer depends on speed or torque, which eliminates the need for speed/load based look-up tables. Figure 11 illustrates the probability of detection at drive idle. As shown on the graph, at every induced misfire, the measured crankshaft angular acceleration drops significantly below the modelled crank acceleration, causing the Misfire Detection Metric (MDM) to spike above the preset threshold. By comparing the locations of programmed and detected misfire flags, in the first and the fourth strips respectively, one can see that the algorithm is capable of detecting every induced misfire at this condition.

Figures 12A and 13A show similar results as those in Figure 11, except at 35 mph and 45 mph driving conditions, respectively. A portion of the time period shown in Figure 12A is zoomed in and shown in Figure 12B to more clearly illustrate the difference between modelled crank

acceleration and measured crank acceleration for three of the induced misfires. Similarly, a portion of Figure 13A is zoomed-in and shown in Figure 13B. The graphs clearly demonstrate that every induced misfire is successfully detected under these conditions.

Validation tests are also conducted over a transient cycle simulating real-world driving conditions. Figure 14 illustrates an example of the detection results. As before, by comparing the locations of programmed and detected misfire flags, one can see that the strategy successfully detected all induced misfire under those test conditions. In short, this torque model based approach proves to be a very good method for detecting misfires in a dynamic skip fire engine.

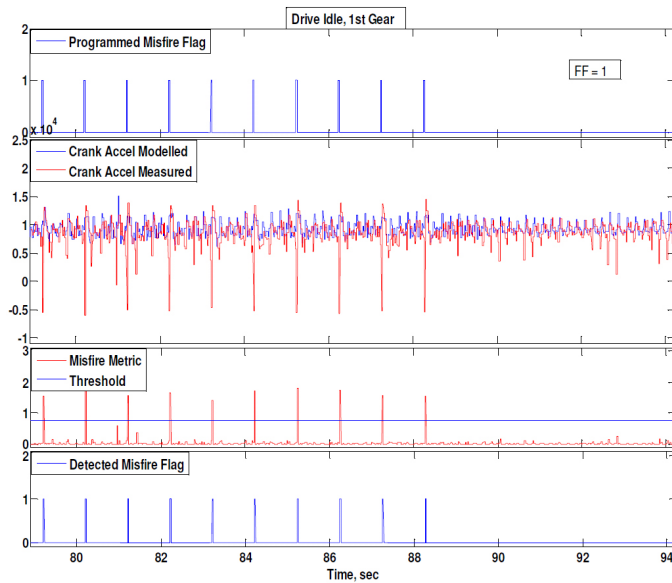


Figure 11. Detection of induced misfire at drive idle

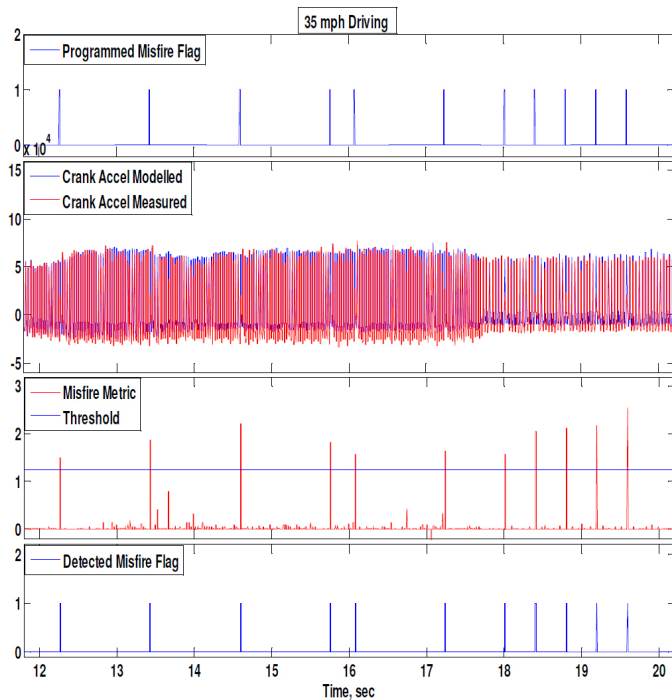


Figure 12A. Detection of induced misfires at 35 mph

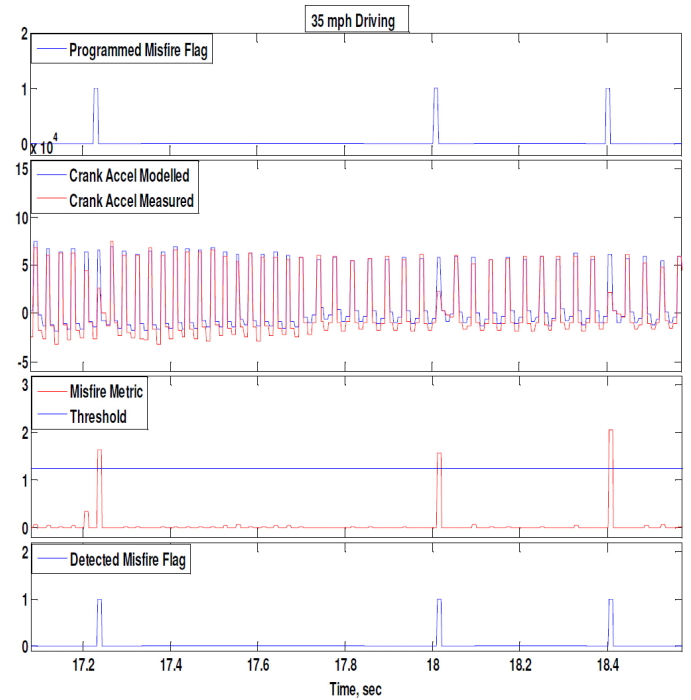


Figure 12B. Detection of induced misfires at 35 mph (zoom-in)

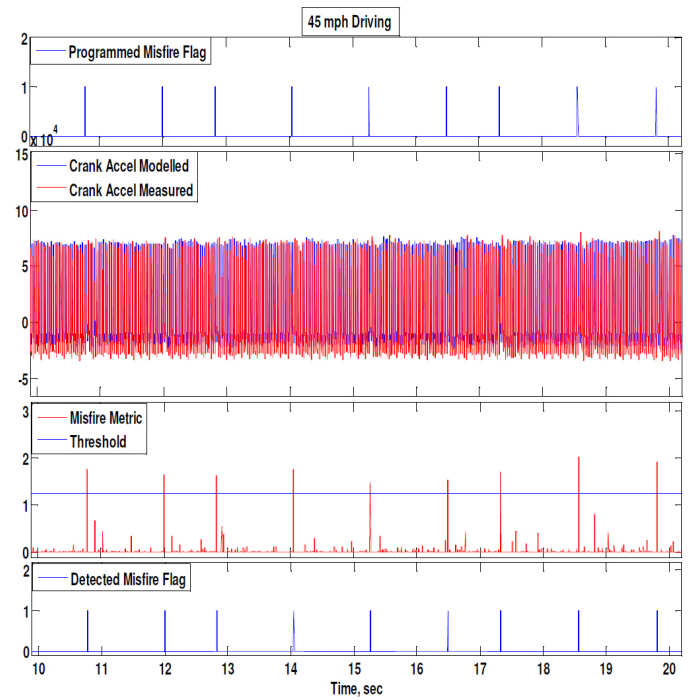


Figure 13A. Detection of induced misfires at 45 mph

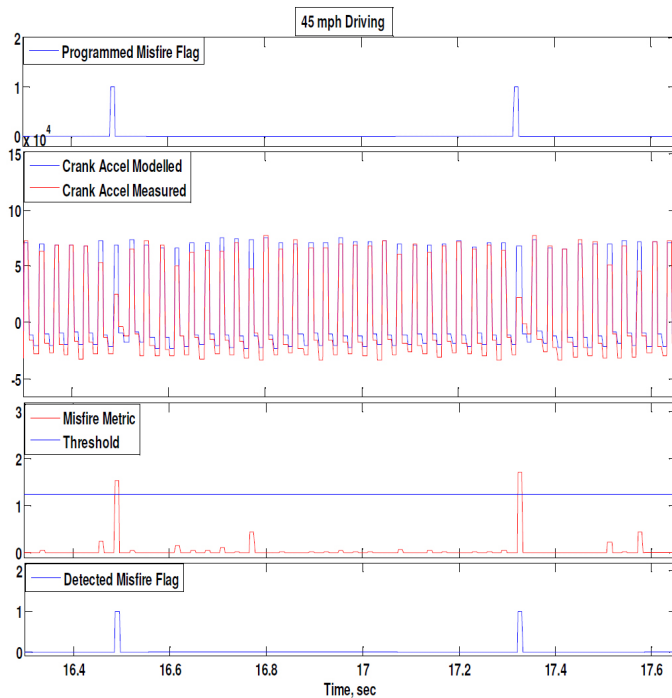


Figure 13B. Detection of induced misfires at 45 mph (zoom-in)

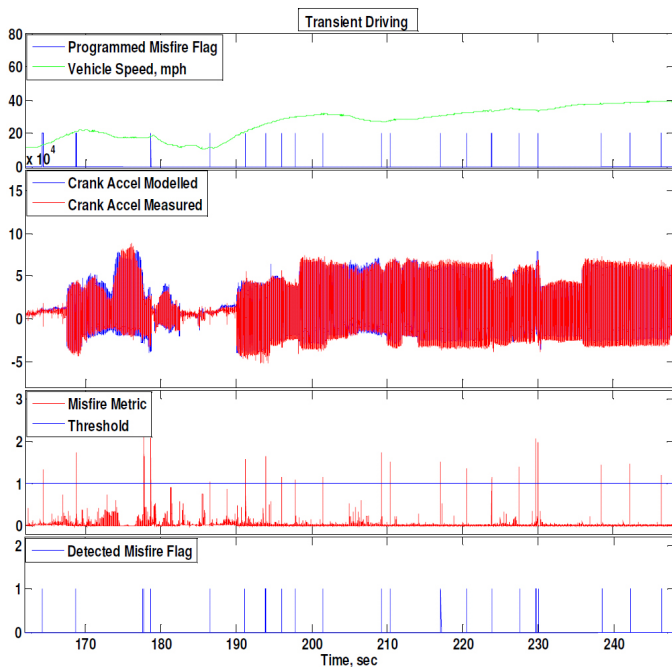


Figure 14. Detection of induced misfire during transient driving

## SUMMARY/CONCLUSIONS

In order to adopt dynamic skip fire technology for automotive applications, a misfire detection algorithm has to be developed to meet OBD-II requirements. This paper presents two promising approaches for detecting misfire. The first method utilizes crankshaft angular acceleration with the addition of cylinder skip or fire status. The method determines a 3-cylinder firing pattern based on the fire/skip status of 3 consecutive cylinders in the firing order, the cylinder of interest and the two adjacent cylinders. The firing pattern is used to determine whether a misfire occurred. If the cylinder of interest was skipped, obviously no

misfire occurred. If the cylinder of interest was fired, the misfire threshold is varied depending on the fire/skip pattern of the adjacent cylinders. The approach has been demonstrated to provide a reasonably high probability of detection for most speed and load regions, although significant calibration is needed to calibrate the threshold tables.

The second method is based on a torque model which incorporates a multi-cylinder pressure model. The cylinder pressure, indicated torque, and crankshaft angular acceleration are modeled by simple relations that are relatively easy to calibrate. A new dimensionless metric is introduced to amplify the differences between measured and modelled crank accelerations. The metric yields a high signal to noise ratio providing a means for robust misfire detection. Validation tests have been carried out both on an engine dynamometer and two vehicles under steady state and transient conditions. The results indicate this is an excellent approach for detecting misfire in a dynamic skip fire engine.

## REFERENCES

1. Wilcutts, M., Switkes, J., Shost, M., and Tripathi, A., "Design and Benefits of Dynamic Skip Fire Strategies for Cylinder Deactivated Engines," *SAE Int. J. Engines* 6(1):278-288, 2013, doi:10.4271/2013-01-0359.
2. Serrano, J., Routledge, G., Lo, N., Shost, M. et al., "Methods of Evaluating and Mitigating NVH when Operating an Engine in Dynamic Skip Fire," *SAE Int. J. Engines* 7(3):1489-1501, 2014, doi:10.4271/2014-01-1675.
3. Merksiz, J., Bogus, P., and Grzeszczyk R., "Overview of Engine Misfire Detection Methods Used in On-Board Diagnostics", *Journal of Kones, Combustion Engines*, Vol 8, No 1-2, 2001
4. Chatterjee, S. and Sivasubrahmaniyan, A., "Comparison of Misfire Detection Technologies in Spark-ignition Engines for Meeting On-Board Diagnostic Regulation," SAE Technical Paper 2013-01-2884, 2013, doi:10.4271/2013-01-2884.
5. Bue, F., Stefano, A., Giaconia, C., and Pipitone, E., "Misfire Detection System based on the Measure of Crankshaft Angular Velocity," *Advanced Microsystems for Automotive Applications*, 2007, pp149 - 161.
6. Baghi Abadi, M., Hajnayeb, A., Hosseingholizadeh, A., and Ghasemloonia, A., "Single and Multiple Misfire Detection in Internal Combustion Engines Using Vold-Kalman Filter Order-Tracking," SAE Technical Paper 2011-01-1536, 2011, doi:10.4271/2011-01-1536.
7. Shiao Y. and Moskwa, J., "Cylinder Pressure and Combustion Heat Release Estimation for SI Engine Diagnostics using Nonlinear Sliding Observers", *IEEE Transactions on Control Systems Technology*, Vol 3. No. 1 March 1995.
8. Ball, J., Bowe, M., Stone, C., and McFadden, P., "Torque Estimation and Misfire Detection using Block Angular Acceleration," SAE Technical Paper 2000-01-0560, 2000, doi:10.4271/2000-01-0560.
9. Eriksson, L. and Andersson, I., "An Analytic Model for Cylinder Pressure in a Four Stroke SI Engine," SAE Technical Paper 2002-01-0371, 2002, doi:10.4271/2002-01-0371.
10. Heywood, J., *Internal Combustion Engine Fundamentals*, April 1988
11. Matekunas, F., *Engine combustion control with ignition timing by pressure ratio management*. US Pat. 4622939, 1986
12. Zweiri, Y., Whidborne, J. and Seneviratne, L., "Instantaneous friction components model for transient engine operation," *Proc. Inst. Mech. Eng. Part J. Automob. Eng.*, vol. 214, no. 7, pp. 809-824, Jul. 2000.
13. Bai, S., Maguire, J.M., and Peng, H., "Dynamic Analysis and Control System Design of Automatic Transmissions," (Warrendale, SAE International, 2013), ISBN 978-0-7680-7604-2.

## CONTACT INFORMATION

Kevin Chen:

[Chenk@tulatech.com](mailto:Chenk@tulatech.com)

## **ACKNOWLEDGMENTS**

The authors would like to give special thanks to Charles Loucks for his early contributions, Xin Yuan for providing the Automated Misfire Generation software, and Chris Chandler, Darin Zimlinghaus, Casey Horner and Matthew Herndon for their assistance in conducting the testing throughout the project.

## **DEFINITIONS/ABBREVIATIONS**

**AFM** - Active Fuel Management

**APC** - Air Charge per Cylinder

**BSFC** - Brake Specific Fuel Consumption

**CAFE** - Corporate Average Fuel Economy

**CARB** - California Air Resources Board

**DSF** - Dynamic Skip Fire

**EVO** - Exhaust Valve Opening

**FTP** - Federal Test Procedure

**IMEP** - Indicated Mean Effective Pressure

**IVC** - Intake Valve Closing

**MAP** - Intake Manifold Absolute Pressure

**MDM** - Misfire Detection Metric

**OBD** - On-Board Diagnostics

**PMEP** - Pumping Mean Effective Pressure

**TCC** - Torque Converter Clutch